

# Possible Ordered States in the 2D Extended Hubbard Model

Masakazu MURAKAMI\*

*Institute for Solid State Physics, University of Tokyo, Roppongi, Minato-ku, Tokyo 106-8666*

(Received December 14, 1999)

Possible ordered states in the 2D extended Hubbard model with on-site ( $U > 0$ ) and nearest-neighbor ( $V$ ) interaction are examined near half filling, with emphasis on the effect of finite  $V$ . First, the phase diagram at absolute zero is determined in the mean field approximation. For  $V < 0$ , a state where  $d_{x^2-y^2}$ -wave superconductivity (dSC), commensurate spin-density-wave (SDW) and  $\pi$ -triplet pair coexist is seen to be stabilized. Here, the importance of  $\pi$ -triplet pair on the coexistence of dSC and SDW is indicated. This coexistent state is hampered by the phase separation (PS), which is generally expected to occur in the presence of finite-range attractive interaction, but survives. For  $V > 0$ , a state where commensurate charge-density-wave (CDW), SDW and ferromagnetism (FM) coexist is seen to be stabilized. Here, the importance of FM on the coexistence of CDW and SDW is indicated. Next, in order to examine the effects of fluctuation on each mean field ordered state, the renormalization group method for the special case that the Fermi level lies just on the saddle points,  $(\pi, 0)$  and  $(0, \pi)$ , is applied. The crucial difference from the mean field result is that superconductivity can arise even for  $U > 0$  and  $V \geq 0$ , where the superconducting gap symmetry is  $d_{x^2-y^2}$ -wave for  $U > 4V$  and  $s$ -wave for  $U < 4V$ . Finally, the possibilities that the mean field coexistent states survive in the presence of fluctuation are discussed.

KEYWORDS: 2D extended Hubbard model, coexistent state, d-wave superconductivity, s-wave superconductivity, spin-density wave, charge-density wave, ferromagnetism,  $\pi$ -triplet pair,  $\eta$ -singlet pair, phase separation

## §1. Introduction

In connection with the studies of the copper oxide high- $T_c$  superconductors with  $\text{CuO}_2$  planes, the electronic states in two-dimensional systems has been intensively studied. Especially, the possibility of various ordered states has been discussed. One characteristic feature is the proximity of superconductivity and antiferromagnetism. In our previous work (hereafter referred to as I),<sup>1)</sup> we have shown in the mean field approximation that the coexistent state with  $d$ -wave superconductivity (dSC), commensurate spin-density-wave (SDW) and  $\pi$ -triplet pair can be stabilized near half filling by *repulsive* backward scattering ('Umklapp' and 'exchange') processes between electrons around the saddle points  $(\pi, 0)$  and  $(0, \pi)$ . As we shall show later, this model with such a particular type of interaction have similar features to those in a square lattice model with on-site *repulsion*  $U > 0$  and nearest-neighbor *attraction*  $V < 0$ , i.e., an *extended Hubbard model*.<sup>2)</sup> Therefore, it is interesting to examine in more detail the possibility of the above coexistent state by use of this model. At the same time, the extended Hubbard model with both on-site and nearest-neighbor *repulsion* ( $U > 0$  and  $V > 0$ ), is also of physical interest. In the 2D extended Hubbard model for  $U > 0$ , it has been shown based on the mean field approximation that extended- $s$ -,  $p$ - and  $d$ -wave superconductivity can arise depending on the electron density

$n$  for  $V < 0$ ,<sup>2,3,4,5)</sup> and commensurate charge- and spin-density wave (CDW and SDW) can appear at half filling  $n = 1$  for  $V > 0$ .<sup>2,3)</sup> However, the property of the ground state for finite carrier doping and the relationship among various order parameters, especially between dSC and SDW, have not been understood yet, even in the mean field approximation. From these points of view, we will study possible ordered states, especially possible coexistence of different orders, in the 2D extended Hubbard model on a square lattice near half filling for  $U > 0$  and  $V \neq 0$ , with emphasis on electrons around the saddle points  $(\pi, 0)$  and  $(0, \pi)$ .

In §2, the extended Hubbard model is introduced and its relationship to our previous model used in I is referred to. In §3, the phase diagram at absolute zero,  $T = 0$ , is determined in the mean field approximation. In §4, the effects of fluctuation on the mean field ordered states are examined based on the renormalization method applicable only for the special case that the saddle points  $(\pi, 0)$  and  $(0, \pi)$  lie just on the Fermi surface.

## §2. Extended Hubbard Hamiltonian

The extended Hubbard Hamiltonian,  $H = H_0 + H_U + H_V$ , is written as follows:

$$H_0 = \sum_{p\sigma} \xi_p c_{p\sigma}^\dagger c_{p\sigma}, \quad (2.1a)$$

$$H_U = U \sum_i n_{i\uparrow} n_{i\downarrow} = \frac{U}{N} \sum_q n_{q\uparrow} n_{-q\downarrow}, \quad (2.1b)$$

\* E-mail: murakami@swan.issp.u-tokyo.ac.jp

$$H_V = \frac{V}{2} \sum_{i\hat{\rho}} n_i n_{i+\hat{\rho}} = \frac{1}{N} \sum_q V_q n_q n_{-q}, \quad (2.1c)$$

where  $\sigma$  is the spin index taking a value of  $+1$  ( $-1$ ) for  $\uparrow$  ( $\downarrow$ ) spin, and the opposite spin to  $\sigma$  is denoted by  $\bar{\sigma} \equiv -\sigma$ .  $N$  is the total number of lattice sites,  $\xi_p = \epsilon_p - \mu$  is the one-particle energy dispersion relative to the chemical potential  $\mu$ , including nearest-neighbor- ( $t$ ) and next-nearest-neighbor- ( $t'$ ) hopping integrals,

$$\epsilon_p = -2t(\cos p_x + \cos p_y) - 4t' \cos p_x \cos p_y, \quad (2.1d)$$

$n_q = \sum_{\sigma} n_{q\sigma} = \sum_{k\sigma} c_{k\sigma}^{\dagger} c_{k+q\sigma}$ ,  $\hat{\rho} = \pm\hat{x}, \pm\hat{y}$  is the unit lattice vector and

$$V_q = V(\cos q_x + \cos q_y). \quad (2.1e)$$

The energy dispersion  $\epsilon_p$  has two independent saddle points,  $(\pi, 0)$  and  $(0, \pi)$ . In this paper, we fix  $t'/t = -1/5$  with  $t > 0$ , in which case the Fermi surface in the absence of interaction approaches  $(\pi, 0)$  and  $(0, \pi)$  as the hole doping rate,  $\delta \equiv 1 - n$ , is increased from half filling,  $\delta = 0$ .

Here, we examine the relationship between the 'g-ology' model used in I and the present extended Hubbard model.<sup>6</sup> In I, we have treated the backward scattering with large momentum transfer between electrons around  $(\pi, 0)$  and  $(0, \pi)$ , i.e., 'Umklapp' ( $g_{3\perp}$ ) and 'exchange' ( $g_{1\perp}$ ) processes, and considered three types of the scattering processes, i.e., (1) Cooper-pair, (2) density-wave and (3)  $\pi$ -pair channels.<sup>1</sup> (Here we denote the Hamiltonian for these channels as  $H_1$ ,  $H_2$  and  $H_3$ .) Especially for the repulsive case,  $g_{3\perp} > 0$  and  $g_{1\perp} > 0$ , we have shown that the coexistent state with dSC, SDW and  $\pi$ -triplet pair can be stabilized near half filling at low temperature. However, the above effective interaction is too simplified in that (a) forward scattering processes are not included and (b) the  $k$ -dependence of interaction is ignored. Therefore, by transforming  $H_i$  ( $i = 1, 2, 3$ ), into real-space representation, we will obtain a well-defined model on a square lattice. If we keep on-site and nearest-neighbor density-density Coulomb interaction, we obtain

$$H_1 \sim \frac{g_{3\perp}}{2N} \left\{ \sum_i n_{i\uparrow} n_{i\downarrow} - \alpha \sum_{\langle ij \rangle} \sum_{\sigma} n_{i\sigma} n_{j\bar{\sigma}} \right\}, \quad (2.2a)$$

$$H_2 \sim \frac{g_{\perp}}{2N} \left\{ \sum_i n_{i\uparrow} n_{i\downarrow} - \sum_{\langle ij \rangle} \sum_{\sigma} n_{i\sigma} n_{j\bar{\sigma}} \right\}, \quad (2.2b)$$

$$H_3 \sim \frac{g_{1\perp}}{2N} \left\{ \sum_i n_{i\uparrow} n_{i\downarrow} - \alpha \sum_{\langle ij \rangle} \sum_{\sigma} n_{i\sigma} n_{j\bar{\sigma}} \right\}, \quad (2.2c)$$

where  $g_{\perp} \equiv g_{3\perp} + g_{1\perp}$ ,  $\langle ij \rangle$  stands for a bond connecting site  $i$  and its nearest-neighbor site  $j$  and  $\alpha = 16/\pi^4 \sim 0.164$ . Each  $H_i$  is seen to describe on-site *repulsion* and nearest-neighbor *attraction* for  $g_{3\perp}, g_{1\perp} > 0$ . Therefore, also in the extended Hubbard model for  $U > 0$  and  $V < 0$ , the coexistent state with dSC, SDW and  $\pi$ -triplet pair is expected to be stabilized.

### §3. Mean Field Analysis

First, we determine the phase diagram at absolute zero,  $T = 0$ , near half filling in the mean field approxima-

tion. We fix the electron density to  $n = 0.9$ . With this choice of parameters, the Fermi surface of noninteracting electrons is of the YBCO- or BSCCO-type and lies close to the saddle points  $(\pi, 0)$  and  $(0, \pi)$ , as shown in Fig. 1.

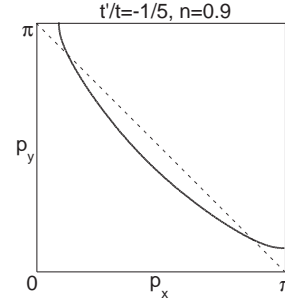


Fig. 1. The Fermi surface in the absence of interaction for  $t'/t = -1/5$  and  $n = 0.9$ .

#### 3.1 Nearest-Neighbor Attraction $V < 0$

We start with the case  $V < 0$ . As we saw in §2, the ordered states with dSC, SDW (= antiferromagnetism, AF) and  $\pi$ -triplet pair is expected. We consider the following order parameters,

$$\langle c_{i\sigma} c_{i+\hat{\rho}, \bar{\sigma}} \rangle \equiv \sigma s_{\hat{\rho}} + q_{\hat{\rho}} \cos(QR_i), \quad (3.1a)$$

$$\langle n_{i\sigma} \rangle \equiv \frac{n}{2} + \sigma m \cos(QR_i), \quad (3.1b)$$

where  $Q = (\pi, \pi)$ ,  $s_{-\hat{\rho}} = s_{\hat{\rho}}$  and  $q_{-\hat{\rho}} = q_{\hat{\rho}}$ .  $s_{\hat{\rho}}$  ( $q_{\hat{\rho}}$ ) stands for a spin-singlet (triplet) pair of two electrons with a total momentum 0 ( $Q$ ) and total spin  $S = 0$  ( $S = 1$  and  $S_z = 0$ ), i.e., Cooper-pair ( $\pi$ -triplet pair), and  $m$  for the local staggered spin moment. We take  $s_{\hat{x}} = -s_{\hat{y}} = s_0 = \text{real}$  and  $q_{\hat{x}} = -q_{\hat{y}} = q_0 = \text{real}$ , i.e., consider  $d_{x^2-y^2}$  wave pairing, which is favored near half filling.<sup>2</sup> While  $s_0$  describes dSC,  $q_0$  describes an electron-pair of  $p_x - p_y$ -wave symmetry.<sup>7,8</sup> This can be easily seen by writing the operator of  $\pi$ -triplet pair in  $k$ -space,

$$\hat{O}_{\pi} \equiv \frac{1}{\sqrt{2}} \sum_{p\sigma} w_p c_{-p+Q\bar{\sigma}} c_{p\sigma}, \quad (3.2a)$$

$$= \frac{1}{\sqrt{2}} \sum_{p\sigma} w_{\frac{Q}{2}+p} c_{\frac{Q}{2}-p\bar{\sigma}} c_{\frac{Q}{2}+p\sigma}, \quad (3.2b)$$

where  $w_p \propto \cos p_x - \cos p_y$  is the  $d_{x^2-y^2}$ -wave factor and  $\langle \hat{O}_{\pi} \rangle \propto q_0$ . The orbital function as a function of the *relative* momentum  $p$  of two electrons,  $w_{\frac{Q}{2}+p}$ , is proportional to  $\sin p_x - \sin p_y$ .

The order parameter in the mean field Hamiltonian are given as follows in terms of  $s_0$ ,  $q_0$  and  $m$ ,

$$\Delta_{dSC} = -2|V|s_0, \quad \Delta_{\pi} = -2|V|q_0, \quad (3.3a)$$

$$\Delta_{SDW} = Um, \quad (3.3b)$$

where  $\Delta_{dSC}$  and  $\Delta_{\pi}$  include only  $V$  because  $s_{\hat{\rho}}$  and  $q_{\hat{\rho}}$  are defined on a bond, and  $\Delta_{SDW}$  does not include  $V$  because  $\langle n_i \rangle = \sum_{\sigma} \langle n_{i\sigma} \rangle$  is independent of  $m$ .

The pure  $\pi$ -triplet pairing state with  $\Delta_{\pi} \neq 0$  and  $\Delta_{dSC} = \Delta_{SDW} = 0$  is always energetically unfavorable

compared with the pure dSC state with  $\Delta_{dSC} \neq 0$  and  $\Delta_{SDW} = \Delta_\pi = 0$ . However, since the coexistence of dSC and SDW ( $\Delta_{dSC} \neq 0$  and  $\Delta_{SDW} \neq 0$ ) generally results in nonzero  $t_0$  (and nonzero  $\Delta_\pi$  here), the self-consistency of mean field calculation requires the consideration of  $\pi$ -triplet pair into account from the outset.<sup>1,9)</sup> The important fact that the coexistence of spin-singlet Cooper-pair and SDW always leads to nonzero spin-triplet pair amplitude with finite total momentum had been recognized by Psaltakis *et al.* in a slightly different context.<sup>10)</sup> The close relationship among the order parameters of dSC, SDW and  $\pi$ -triplet pair is discussed in Appendix A.

The mean field phase diagram in the plane of  $U$  and  $|V|$  is shown in Fig. 2. While the dSC state is stabilized for small  $U/t$ , the coexistent state with dSC, SDW and  $\pi$ -triplet pair is possible for large  $U/t$ , and the phase boundary between these two states is shown by solid line. Although the pure  $\pi$ -triplet pairing state cannot be stabilized,  $\pi$ -triplet pair can condensate as a result of the coexistence of dSC and SDW. Since there is *attractive* interaction for spin-triplet channel in the present model, the coexistent region of dSC and SDW is widened by the inclusion of  $\pi$ -triplet pair. We note that the Fermi surface remains in the SDW state near half filling. As we saw in I, when SDW appears first as the temperature is lowered, the coexistent state can be stabilized at lower temperature, especially at  $T = 0$ , near half filling.

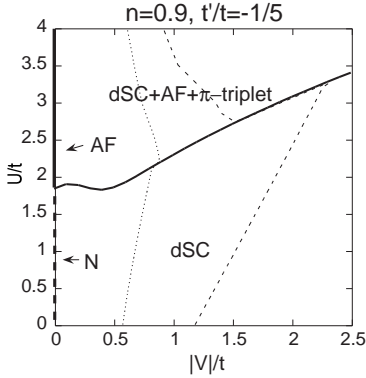


Fig. 2. The mean field phase diagram at  $T = 0$  for  $U > 0$ ,  $V < 0$ ,  $n = 0.9$  and  $t'/t = -1/5$ . Solid line stands for the boundary between the coexistent state and dSC state in the mean field approximation. Dotted and broken lines stand for the boundary in the right side of which the phase separation occurs in the random phase approximation for  $V' = 0$  and  $V' = |V|/2$ , respectively, where  $V'$  is the next-nearest-neighbor density-density interaction.  $N$  stands for the normal state.

Generally, in the presence of finite-range attractive density-density interaction, the system can be hampered by the phase separation (PS). In order to examine the PS transition, we calculate the charge compressibility,  $\kappa$ , given by static and uniform charge susceptibility, in the ground state, i.e., dSC or coexistent state. This phase boundary is determined from  $\kappa^{-1} = 0$ . Here we use the random phase approximation (RPA), and take the RPA diagram, shown in Fig. 3, into account. The explicit form of  $\kappa$  in the RPA is shown in Appendix B. The PS transition line is shown in Fig. 2 by dot-

ted line. It is seen that the coexistent state is severely suppressed by PS but survives. This PS is expected to be suppressed if we take the long-range Coulomb repulsion into account. Here, for simplicity, we consider the *next*-nearest-neighbor density-density repulsion  $V' > 0$ ,

$$H_{V'} = \frac{V'}{2} \sum_{i\hat{l}} n_i n_{i+\hat{l}} = \frac{1}{N} \sum_q V'_q n_q n_{-q}, \quad (3.4a)$$

$$V'_q = 2V' \cos q_x \cos q_y, \quad (3.4b)$$

where  $\hat{l} = \pm(\hat{x} + \hat{y}), \pm(\hat{x} - \hat{y})$ , and incorporate  $V'$  into the RPA calculation, i.e., we replace  $V_q$  with  $V_q + V'_q$ . We note that this replacement, which does not alter the mean field equations, can bring about the nontrivial effect on  $\kappa$  in the coexistent state, from eq. (B.10a). For  $V' = |V|/2$ , the PS transition line is shifted, as shown in Fig. 2, from dotted line to broken line. It is seen that the long-range Coulomb interaction does lead to the suppression of the PS, which is less prominent in the coexistent state than in the dSC state.

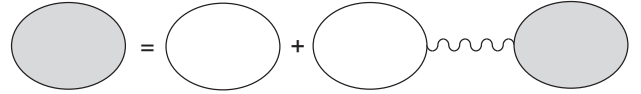


Fig. 3. The RPA diagram for charge susceptibility.

The calculation of  $\kappa$  in the RPA had been carried over by Micnas *et al.*,<sup>2)</sup> *only* in the normal state. Dagotto *et al.*<sup>3)</sup> have shown based on quantum Monte Carlo (QMC) simulation that (1) PS drastically reduces the size of the mean field dSC region and (2) the enhancement of  $d_{x^2-y^2}$  pairing correlation itself is not found. This QMC result of (2) is different from the present mean field calculation. We note that this QMC calculation is limited to the case of half filling  $n = 1$  and relatively high temperature  $T = t/6$ .

The coexistence of dSC and SDW near half filling has been found also in the  $t$ - $J$  model in the slave-boson mean field approximation<sup>11)</sup> and by use of variational Monte Carlo calculation (VMC),<sup>12,13,14)</sup> and in the repulsive Hubbard model ( $V = 0$ ) by use of VMC.<sup>13,15)</sup> In these studies, however,  $\pi$ -triplet pair has not been taken into account. The effect of  $\pi$ -triplet pair on the coexistence of dSC and SDW has been recently examined by Arrachea *et al.*<sup>9)</sup> based on a generalized Hubbard model. In the repulsive Hubbard model, the nearest-neighbor hopping term is modified as the correlated one,

$$H_{ch} = - \sum_{\langle ij \rangle \sigma} \left\{ c_{i\sigma}^\dagger c_{j\sigma} + c_{j\sigma}^\dagger c_{i\sigma} \right\} \\ \times \left\{ t_{AA}(1 - n_{i\bar{\sigma}})(1 - n_{j\bar{\sigma}}) + t_{BB}n_{i\bar{\sigma}}n_{j\bar{\sigma}} \right. \\ \left. + t_{AB}[n_{i\bar{\sigma}}(1 - n_{j\bar{\sigma}}) + (1 - n_{i\bar{\sigma}})n_{j\bar{\sigma}}] \right\}, \quad (3.5)$$

where three hopping integrals,  $t_{AA}$ ,  $t_{BB}$  and  $t_{AB}$ , incorporate many-body effects into one-particle hopping processes phenomenologically.  $t_{AA}$  and  $t_{BB}$  do not change the number of doubly occupied sites, and  $t_{AB}$  does, as

shown in Fig. 4. It is to be noted that  $H_{ch}$  can be rewritten as

$$H_{ch} = \sum_{\langle ij \rangle \sigma} \left\{ c_{i\sigma}^\dagger c_{j\sigma} + c_{i\sigma}^\dagger c_{j\sigma} \right\} \times \left\{ -t + t_2(n_{i\bar{\sigma}} + n_{j\bar{\sigma}}) + t_3 n_{i\bar{\sigma}} n_{j\bar{\sigma}} \right\}, \quad (3.6a)$$

where

$$t \equiv t_{AA}, \quad t_2 \equiv t_{AA} - t_{AB}, \quad t_3 \equiv 2t_{AB} - t_{AA} - t_{BB}. \quad (3.6b)$$

The  $t_2$  term can be also deduced from the bare Coulomb interaction<sup>16, 17, 18)</sup> or by including the effects of phonon in the antiadiabatic approximation  $M \rightarrow 0$  (where  $M$  is the phonon mass),<sup>19)</sup> and the  $t_3$  term describes the three-body interaction. Arrachea *et al.* have shown in the mean field approximation for  $t_{AB} > t_{AA} = t_{BB}$  (i.e.,  $t_2 < 0$  and  $t_3 = -2t_2 > 0$ ) and  $t' = 0$  that the coexistence of dSC and SDW is possible but prevented by  $\pi$ -triplet pair (and ruled out for large  $U$ ), due to *repulsive* spin-triplet pairing interaction. Hence, the effect of  $\pi$ -triplet pair on the coexistence of dSC and SDW is different from that in the present extended Hubbard model.

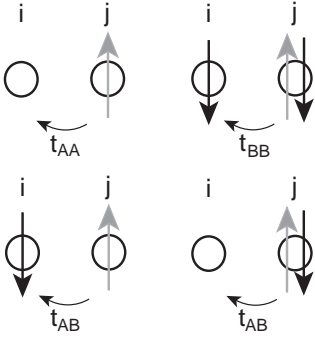


Fig. 4. The correlated hopping processes.

### 3.2 Nearest-Neighbor Repulsion $V > 0$

Next we treat the case  $V > 0$ . In this case, not only charge- and spin-density-wave states (CDW and SDW), but also orbital antiferromagnetic (OAF) and spin nematic (SN) states, in which the local staggered currents of charge and spin circulate, respectively,<sup>20, 21, 22, 23)</sup> are expected.<sup>24)</sup> Here we include ferromagnetism (FM) for the reason as we shall describe later. The order parameters are

$$\langle n_{i\sigma} \rangle \equiv \frac{n}{2} + \sigma f + (p + \sigma m) \cos(QR_i), \quad (3.7a)$$

$$\langle c_{i\sigma}^\dagger c_{i+\hat{\rho},\sigma} \rangle \equiv (g_{\hat{\rho}} + \sigma l_{\hat{\rho}}) \cos(QR_i), \quad (3.7b)$$

where  $f$ ,  $p$  and  $m$  are real,  $g_{-\hat{\rho}} = -g_{\hat{\rho}}^*$  and  $l_{-\hat{\rho}} = -l_{\hat{\rho}}^*$ .  $f$ ,  $p$  and  $m$  describes FM, CDW and SDW, respectively. We take  $g_{\hat{\rho}}$  and  $l_{\hat{\rho}}$  to be of  $d_{x^2-y^2}$  wave symmetry, which is favored near half filling.<sup>24)</sup> In this case,  $g_{\hat{\rho}}$  and  $l_{\hat{\rho}}$  become pure imaginary,  $g_{\pm\hat{x}} = -g_{\pm\hat{y}} = ig$  and  $l_{\pm\hat{x}} = -l_{\pm\hat{y}} = il$ , where  $g$  and  $l$  are real. The states with  $g \neq 0$  and  $l \neq 0$  are called as OAF and SN ones,<sup>20, 21, 22, 23)</sup> respectively, in which there exist the staggered local currents of charge

and spin on a bond  $(i, i + \hat{\rho})$ ,

$$\langle j_{i,i+\hat{x}}^c \rangle = - \langle j_{i,i+\hat{y}}^c \rangle \propto g \cos(QR_i), \quad (3.8a)$$

$$\langle j_{i,i+\hat{x}}^s \rangle = - \langle j_{i,i+\hat{y}}^s \rangle \propto l \cos(QR_i), \quad (3.8b)$$

where

$$j_{i,i+\hat{\rho}}^\nu \equiv i \sum_{\sigma} v_{\nu} (c_{i\sigma}^\dagger c_{i+\hat{\rho},\sigma} - c_{i+\hat{\rho},\sigma}^\dagger c_{i\sigma}), \quad (3.9)$$

and  $v_c = 1$  and  $v_s = \sigma$ . In the OAF (SN) state, the local staggered current of charge (spin) circulates around the plaquettes, as schematically shown in Fig. 5, and the bond-ordered wave (BOW) does not exist, i.e.,  $\langle c_{i\sigma}^\dagger c_{i+\hat{\rho},\sigma} + c_{i+\hat{\rho},\sigma}^\dagger c_{i\sigma} \rangle \equiv 0$ .

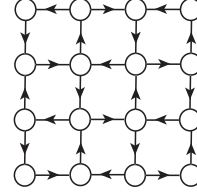


Fig. 5. The OAF (SN) state in which the local staggered charge (spin) current circulates around the plaquettes.

The order parameters in the mean field Hamiltonian are given as follows in terms of  $f$ ,  $p$ ,  $m$ ,  $g$  and  $l$ ,

$$\Delta_{FM} = Uf, \quad (3.10a)$$

$$\Delta_{CDW} = (8V - U)p, \quad \Delta_{SDW} = Um, \quad (3.10b)$$

$$\Delta_{OAF} = 2Vg, \quad \Delta_{SN} = 2Vl, \quad (3.10c)$$

where  $\Delta_{OAF}$  and  $\Delta_{SN}$  include only  $V$  because  $g_{\hat{\rho}}$  and  $l_{\hat{\rho}}$  are defined on a bond, and  $\Delta_{FM}$  does not include  $V$  because  $\langle n_i \rangle = \sum_{\sigma} \langle n_{i\sigma} \rangle$  is independent of  $f$ . The order parameters of CDW, SDW, OAF and SN are closely related to each other, which is shown in Appendix A.

The mean field phase diagram in the plane of  $U$  and  $V$  is shown in Fig. 6. We have found that a coexistent solution with nonzero  $\Delta_{CDW}$ ,  $\Delta_{SDW}$  and  $\Delta_{FM}$  can be stabilized for  $n \neq 1$ . This state is *ferrimagnetic*, as shown in Fig. 7. We note that the coexistence of CDW and SDW ( $\Delta_{CDW} \neq 0$  and  $\Delta_{SDW} \neq 0$ ) generally results in nonzero  $f$  (and nonzero  $\Delta_{FM}$  here), which had been indicated by Dzyaloshinskiĭ<sup>25)</sup> based on a qualitative symmetry analysis. This is the reason why we take FM into account from the outset. With the present choice of parameters, pure FM state with only  $\Delta_{FM} \neq 0$  cannot be stabilized, but FM can arise as a result of the coexistence of CDW and SDW. In the present case, the coexistent region of CDW and SDW is widened by the inclusion of FM. We note that the Fermi surface remains in the CDW or SDW state near half filling.

It is to be noted that neither OAF nor SN can be stabilized solely in the mean field approximation, *independent* of  $t'$ ,  $U$ ,  $V$ ,  $T$  and  $n$ . This conclusion is contrary to that of Chattopadhyay *et al.*<sup>24)</sup> that pure OAF or SN state has lower ground-state energy than pure CDW or SDW state for the half-filled case by introducing finite

$t'$ . Moreover, a state where local-current (OAF or SN) and density-wave (CDW or SDW) coexist cannot be also stabilized.

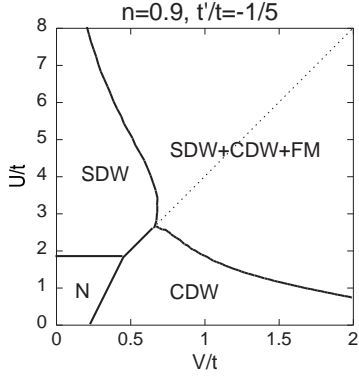


Fig. 6. The mean field phase diagram at  $T = 0$  for  $U > 0$ ,  $V > 0$ ,  $n = 0.9$  and  $t'/t = -1/5$ .

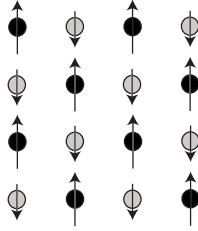


Fig. 7. The ferrimagnetic coexistent state. Each lattice site is shaded according to electron density. The length of each arrow is proportional to the magnitude of local spin moment. Lattice sites with larger local spin moment have higher electron density.

For  $U/t = 4.0$ , the  $V$  dependences of  $\Delta_{CDW}$ ,  $\Delta_{SDW}$ ,  $\Delta_{FM}$  and the difference between the energy of the pure state (CDW for  $U < 4V$  or SDW for  $U > 4V$ ),  $E_p$ , and that of the coexistent state (CDW+SDW+FM),  $E_c$ , are shown in Fig. 8. In the coexistent state with CDW, SDW and FM,  $|\Delta_{SDW}|$  is larger than  $|\Delta_{CDW}|$  for  $U > 4V$  and vice versa for  $U < 4V$ , and the first-order phase transition occurs at  $U = 4V$ . For fixed  $U$ ,  $|\Delta_{FM}|$  rapidly saturates as a function of  $V$ . It is seen that the energy gain in the coexistent state is very small.

The energy dispersion in the ferrimagnetic coexistent state is shown in Fig. 9. There are four energy bands, and the Fermi surface remains as in the CDW or SDW state. However, the lower band of electrons with majority spin (up spin for  $\Delta_{FM} > 0$ ) is fully occupied and the Fermi level crosses only the lower band of electrons with minority spin (down spin for  $\Delta_{FM} > 0$ ). Therefore, this coexistent state is *half metallic*.

The coexistence of CDW and SDW with *same* wave vectors has also been found in a 1D modified Hubbard model for a quarter-filled band in the mean field approximation.<sup>26)</sup> In this coexistent state, the wave vector of charge and spin density,  $q$ , and the phase difference between CDW and SDW,  $\Delta\theta$ , are equal to  $2k_F \equiv \pi/2$  and  $\pi/2$ , respectively, and the magnitude of local spin moment is equal at each site, as shown in Fig. 10. On the other hand, in our coexistent state,  $q = Q \equiv (\pi, \pi)$  and

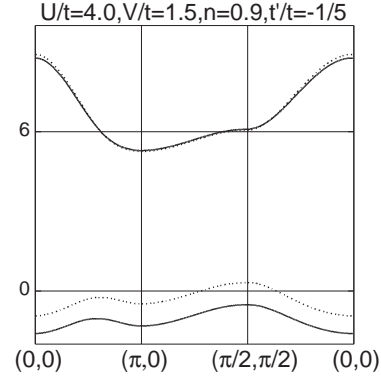


Fig. 9. The energy dispersion relative to the Fermi level in the coexistent state with CDW, SDW and FM for  $U/t = 4.0$ ,  $V/t = 1.5$ ,  $n = 0.9$  and  $t'/t = -1/5$ . Full (dotted) lines stand for that of electrons with up (down) spin, respectively. The lower band of electrons with up spin is fully occupied.

$\Delta\theta = 0$ , and the magnitude of local spin moment is different at each sublattice, as shown in Fig. 7. This *ferrimagnetic* coexistent state is the 2D version of that found in the 3D Hubbard model ( $V = 0$ ) which had been denoted as the special ferrimagnetic (S.F.) state.<sup>27)</sup> In the present 2D case, this coexistent state for  $V = 0$  can be stabilized for  $12 \lesssim U/t \lesssim 14$  (not shown in Fig. 6).



Fig. 10. The coexistent state with  $2k_F$  CDW and  $2k_F$  SDW found in a quarter-filled 1D modified Hubbard model.<sup>26)</sup> Each lattice site is shaded according to electron density. The length of each arrow, proportional to the magnitude of local spin moment, is equal at each site.

#### §4. Renormalization Group Analysis

In the last section, we examined possible ordered states for  $U > 0$  and  $V \neq 0$  in the mean field approximation. In this section, we examine the effects of fluctuation on these ordered states which are not taken into account in the mean field calculation. As a theoretical treatment beyond the mean field level, we adopt the renormalization group (RG) method for the saddle points which has been applied to the Hubbard model ( $V = 0$ ),<sup>28, 29, 25, 30, 31, 32, 33)</sup> and determine the most dominant correlation in the normal state. We also discuss the possibility of the coexistent states beyond the mean field approximation.

##### 4.1 Saddle Point Singularity

We consider the *special* case where the Fermi level in the absence of interaction lies *just* on the saddle points  $Q_A \equiv (\pi, 0)$  and  $Q_B \equiv (0, \pi)$ , i.e.,  $\mu = 4t'$  ( $n \sim 0.83$ ), and focus on electrons at these two saddle points *on the Fermi surface*, just as two Fermi points in 1D electron systems. The Fermi surface is shown in Fig. 11.

First, we examine the behavior of the following



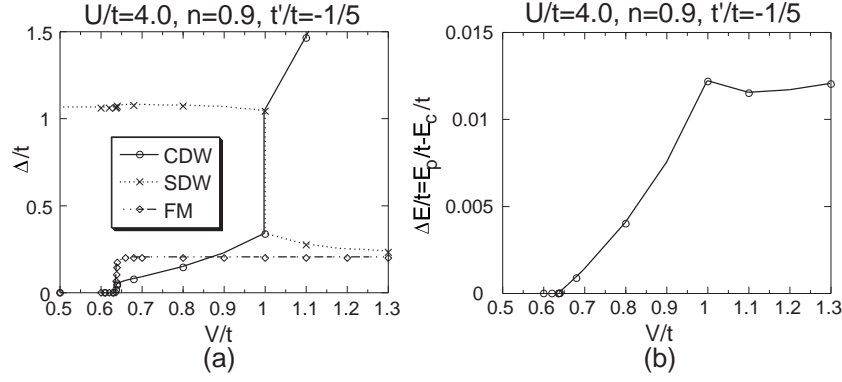


Fig. 8. The  $V$  dependences of (a)  $\Delta_{CDW}$ ,  $\Delta_{SDW}$ ,  $\Delta_{FM}$  and (b) the energy difference  $E_p - E_c$  (scaled by  $t$ ) between the pure state (CDW or SDW) and the coexistent state (CDW+SDW+FM) for  $U/t = 4.0$ ,  $n = 0.9$  and  $t'/t = -1/5$ .

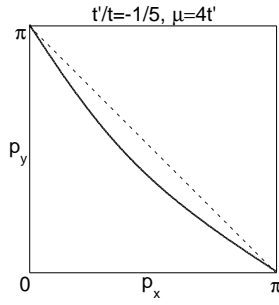


Fig. 11. The Fermi surface in the absence of interaction for  $t'/t = -1/5$  and  $\mu = 4t'$ , in which case  $n \sim 0.83$ .

particle-particle (K) and particle-hole (P) correlation functions,

$$K_{\alpha\alpha'} = \lim_{q \rightarrow 0} \int_{k,\epsilon} G_{\alpha}(k, \epsilon) G_{\alpha'}(-k + q, -\epsilon), \quad (4.1a)$$

$$P_{\alpha\alpha'} = \lim_{q \rightarrow 0} \int_{k,\epsilon} G_{\alpha}(k, \epsilon) G_{\alpha'}(k + q, \epsilon), \quad (4.1b)$$

for  $\alpha, \alpha' = A, B$ , where

$$G_{\alpha}(k, \epsilon) \equiv \frac{1}{i\epsilon - \xi_{Q_{\alpha}+k}}, \quad (4.2)$$

is the one-particle Green function in the absence of interaction for electrons near the saddle point  $Q_{\alpha}$  and

$$\int_{k,\epsilon} \equiv \int_{|k| < k_c} \frac{d^2k}{(2\pi)^2} \int \frac{d\epsilon}{2\pi}, \quad (4.3)$$

where the cutoff around the saddle points,  $k_c$ , is introduced. We note that

$$K_1 \equiv K_{AA} = K_{BB}, \quad K_2 \equiv K_{AB} = K_{BA}, \quad (4.4a)$$

stand for Cooper- and  $\pi$ -pair correlation, respectively, and

$$P_1 \equiv P_{AA} = P_{BB}, \quad P_2 \equiv P_{AB} = P_{BA}, \quad (4.4b)$$

for uniform and staggered density-density correlation, respectively. For  $\mu = 4t'$ , these correlation functions are

logarithmically divergent,

$$K_1 \sim \frac{c}{8\pi^2 t} \log^2 \frac{E_c}{\omega}, \quad P_1 \sim -\frac{c}{4\pi^2 t} \log \frac{E_c}{\omega}, \quad (4.5a)$$

$$K_2 \sim \begin{cases} \frac{c''}{4\pi^2 t} \log \frac{E_c}{\omega} & \text{for } \omega \ll rE_c, \\ -P_1 & \text{for } \omega \gg rE_c, \end{cases} \quad (4.5b)$$

$$P_2 \sim \begin{cases} -\frac{c'}{4\pi^2 t} \log \frac{E_c}{\omega} & \text{for } \omega \ll rE_c, \\ -K_1 & \text{for } \omega \gg rE_c, \end{cases} \quad (4.5c)$$

where  $E_c > 0$  and  $\omega > 0$  ( $\omega \ll E_c$ ) are the ultraviolet and infrared energy cutoff, respectively,

$$c \equiv \frac{1}{\sqrt{1-4r^2}}, \quad (4.6a)$$

$$c' \equiv \log \frac{1 + \sqrt{1-4r^2}}{2r}, \quad (4.6b)$$

$$c'' \equiv \frac{1}{2r} \arctan\left(\frac{2r}{\sqrt{1-4r^2}}\right), \quad (4.6c)$$

and  $r \equiv |t'|/t$ .  $c$ ,  $c'$  and  $c''$  as a function of  $r$  are shown in Fig. 12. Especially for small  $r$ ,

$$c, c'' \sim 1, \quad c' \sim -\log r. \quad (4.7)$$

For  $r > r_c \sim 0.276$ ,  $c > c'$  and  $P_1$  is more divergent than  $P_2$  for  $\omega \rightarrow 0$ . We note  $c'' < \max\{c, c'\}$ , i.e.,  $\pi$ -pair susceptibility  $K_2$  is always less divergent than particle-hole susceptibility. For  $t'/t = -0.2$ ,  $c'' < c < c'$  and they are comparable in magnitude.

#### 4.2 Renormalization Group Method for the Saddle Points

In the last subsection, we saw that the saddle points on the Fermi surface lead to logarithmic divergence of particle-particle and particle-hole correlation functions. This implies that the fluctuation effect becomes strong. In the RG approach, we assume that the single renormalization group variable  $x \equiv \log \frac{E_c}{\omega}$  determine the behavior of the system. The increase of  $x$  represents renormalization towards lower energy scale. For simplicity, we neglect (1) the deformation of the Fermi surface by in-

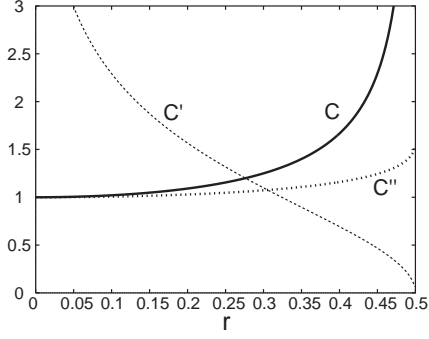


Fig. 12.  $c$ ,  $c'$  and  $c''$  as a function of  $r$ .

teraction and (2)  $k$ -dependence of interaction for small  $|k| < k_c$ , i.e., we consider only eight coupling constants,  $g_{is}$  ( $i = 1, 2, 3, 4$  and  $s = \perp, \parallel$ ). This interaction of the g-ology type is shown in Fig. 13.  $g_1$  and  $g_3$  ( $g_2$  and  $g_4$ ) stand for the backward (forward) scattering processes with large (small) momentum transfer, respectively. Especially,  $g_1$  and  $g_3$  describe 'exchange' and 'Umklapp' processes. In I, only  $g_{1\perp}$  and  $g_{3\perp}$  were treated and taken to be momentum-independent all over the magnetic Brillouin zone.<sup>1)</sup>

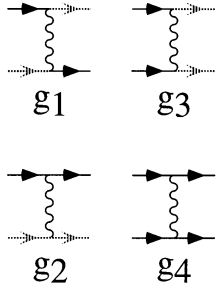


Fig. 13. The scattering processes. Solid and dashed lines stand for electrons near  $Q_A = (\pi, 0)$  and  $Q_B = (0, \pi)$ , respectively.

We start with the renormalization of the couplings in the one-loop approximation. One-loop diagrams are shown in Fig. 14. The scaling equations are

$$g_{1\perp} = -2g_{1\perp}g_{2\perp}\dot{K}_2 - 2g_{1\perp}g_{4\perp}\dot{P}_1 + 2g_{1\perp}(g_{1\parallel} - g_{2\parallel})\dot{P}_2, \quad (4.8a)$$

$$g_{1\parallel} = -2g_{1\parallel}g_{2\parallel}\dot{K}_2 - 2g_{1\parallel}g_{4\parallel}\dot{P}_1 + [2g_{1\parallel}(g_{1\parallel} - g_{2\parallel}) + (g_{1\perp}^2 - g_{1\parallel}^2) + (g_{3\perp}^2 - g_{3\parallel}^2)]\dot{P}_2, \quad (4.8b)$$

$$g_{2\perp} = -(g_{1\perp}^2 + g_{2\perp}^2)\dot{K}_2 - 2g_{4\perp}(g_{1\parallel} - g_{2\parallel})\dot{P}_1 - (g_{2\perp}^2 + g_{3\perp}^2)\dot{P}_2, \quad (4.8c)$$

$$g_{2\parallel} = -(g_{1\parallel}^2 + g_{2\parallel}^2)\dot{K}_2 - 2(g_{4\parallel}g_{1\parallel} - g_{4\perp}g_{2\perp})\dot{P}_1 - (g_{2\parallel}^2 + g_{3\parallel}^2)\dot{P}_2, \quad (4.8d)$$

$$g_{3\perp} = -2g_{3\perp}g_{4\perp}\dot{K}_1 - 2g_{3\perp}(g_{2\perp} + g_{2\parallel} - g_{1\parallel})\dot{P}_2 \quad (4.8e)$$

$$g_{3\parallel} = -2g_{3\parallel}g_{4\parallel}\dot{K}_1 - 2(2g_{3\parallel}g_{2\parallel} - g_{3\perp}g_{1\perp})\dot{P}_2, \quad (4.8f)$$

$$g_{4\perp} = -(g_{3\perp}^2 + g_{4\perp}^2)\dot{K}_1 - [g_{1\perp}^2 + g_{4\perp}^2 + 2g_{2\perp}(g_{1\parallel} - g_{2\parallel})]\dot{P}_1, \quad (4.8g)$$

$$g_{4\parallel} = -(g_{3\parallel}^2 + g_{4\parallel}^2)\dot{K}_1 - [g_{1\parallel}^2 + (2g_{4\parallel}^2 - g_{4\perp}^2) + 2g_{2\parallel}(g_{1\parallel} - g_{2\parallel}) - (g_{2\perp}^2 - g_{2\parallel}^2)]\dot{P}_1, \quad (4.8h)$$

which are to be solved with the initial conditions  $g_{is}(x = x_i) = g_{is}^0$  ( $\dot{\cdot} \equiv d/dx$ ), where  $g_{is}^0$  are the bare coupling constants. For example,  $g_{3\perp}$  has the following form to one loop order,

$$g_{3\perp} = -2g_{3\perp}^0g_{4\perp}^0K_1 - 2g_{3\perp}^0(g_{2\perp}^0 + g_{2\parallel}^0 - g_{1\parallel}^0)P_2. \quad (4.9)$$

By differentiating this equation by  $x$  and replace  $g_{is}^0$  by  $g_{is}$ , i.e., the bare coupling constants by the renormalized ones, we obtain the scaling equation eq. (4.8e).

If we take  $g_{i\perp}^0 = g_{i\parallel}^0$  as the initial conditions, the relation  $g_{i\perp} = g_{i\parallel}$  holds all through the flow. Therefore, the above scaling equations are simplified as follows,<sup>33)</sup>

$$g_1 = -2g_1g_2\dot{K}_2 - 2g_1g_4\dot{P}_1 - 2g_1(g_2 - g_1)\dot{P}_2 \quad (4.10a)$$

$$g_2 = -(g_1^2 + g_2^2)\dot{K}_2 + 2g_4(g_2 - g_1)\dot{P}_1 - (g_2^2 + g_3^2)\dot{P}_2, \quad (4.10b)$$

$$g_3 = -2g_3g_4\dot{K}_1 - 2g_3(2g_2 - g_1)\dot{P}_2, \quad (4.10c)$$

$$g_4 = -(g_3^2 + g_4^2)\dot{K}_1 - [g_1^2 + g_4^2 + -2g_2(g_2 - g_1)]\dot{P}_1. \quad (4.10d)$$

where  $g_i \equiv g_{i\perp} = g_{i\parallel}$ .

The divergence of  $g_{is}(x)$  at a *finite*  $x$  indicates the existence of the strong coupling fixed point, i.e., signals the development of an ordered state, at *finite* energy scale or *finite* temperature. (Strictly speaking, this *finite* onset temperature is an artifact of the present approximation in the 2D systems, and should be interpreted as a crossover temperature, or a critical temperature when finite three-dimensionality is assumed.) The properties of this strong coupling fixed point can be obtained qualitatively from various response functions. The response functions in the one-loop approximation are obtained from one-loop diagrams shown in Fig. 15. The response function,

$$R_\nu = \int_0^\beta d\tau e^{i0\tau} \cdot \frac{1}{N} \langle T_\tau \hat{O}_\nu^\dagger(\tau) \hat{O}_\nu \rangle, \quad (4.11)$$

where  $\nu$  stands for the kind of correlation ( $\nu = \text{dSC}, \text{SDW}, \dots$ ), has the following form to one-loop order,

$$R_\nu = R_\nu^0 + \frac{1}{4}g_\nu^0(R_\nu^0)^2, \quad (4.12)$$

where  $g_\nu^0$  is the coupling constant (linear combination of  $g_{is}^0$ ) and  $R_\nu^0$  is the simple bubble. If we differentiate this equation by  $x$  and replace  $g_\nu^0$ ,  $R_\nu^0$  by the renormalized ones,  $g_\nu$  and  $R_\nu$ , we obtain

$$\dot{R}_\nu = \dot{R}_\nu^0 \left\{ 1 + \frac{1}{2}g_\nu R_\nu \right\}. \quad (4.13)$$

This equation is to be solved with the initial condition that  $R_\nu(x = x_i) \sim 0$ . Since  $\dot{R}_\nu^0$  is positive,  $R_\nu$  can

be divergent for  $g_\nu > 0$  and are suppressed to zero for  $g_\nu < 0$ . In this paper, we consider the response functions shown in Fig 16, where  $\hat{O}_{sSC}$ ,  $\hat{O}_\eta$  and  $\hat{O}_{PS}$  stand for  $s$ -wave Cooper-pair,  $\eta$ -singlet pair with a total momentum  $Q$  and total spin  $S = 0$ ,<sup>34,35)</sup> and uniform charge density, respectively. The most divergent  $R_{PS}$  is interpreted to describe the phase separation (PS). The relationship among these order parameters is discussed in Appendix A. We note that each correlation is treated independently in the above procedure. Therefore, we can determine the most dominant susceptibility in the normal state, and cannot assess the coexistence of different orders.

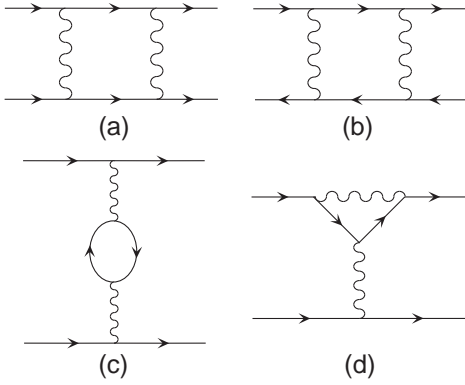


Fig. 14. Diagrams contributing to the one-loop order correction to coupling constants.

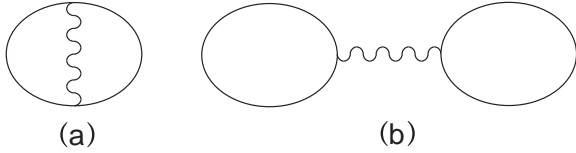


Fig. 15. Diagrams contributing to the one-loop order correction to response functions.

### 4.3 Phase Diagram

We solve the scaling equations, eq. (4.8) and (4.13), with the initial conditions,

$$g_{1\perp}^0 = g_{3\perp}^0 \equiv U + 2V_Q = U - 4V, \quad (4.14a)$$

$$g_{2\perp}^0 = g_{4\perp}^0 \equiv U + 2V_0 = U + 4V, \quad (4.14b)$$

$$g_{1\parallel}^0 = g_{3\parallel}^0 \equiv 2V_Q = -4V, \quad (4.14c)$$

$$g_{2\parallel}^0 = g_{4\parallel}^0 \equiv 2V_0 = 4V, \quad (4.14d)$$

at  $x = x_i$ . Here, we take  $x_i \equiv 0$  and  $R_\nu(x_i) \equiv 0$  for simplicity, although the solution of the scaling equations depends on the value of  $x_i$  and  $R_\nu(x_i)$ .

Before we show our results, we refer to previous results for  $U > 0$  and  $V = 0$  obtained by many authors.  $H_U$

$\nu$	$\hat{O}_\nu$	$R_\nu^0$	$g_\nu$
dSC	$\frac{1}{\sqrt{2}} \sum_{p\sigma} \sigma w_p c_{-p\bar{\sigma}} c_{p\sigma}$	$4K_1$	$g_{3\perp} - g_{4\perp}$
sSC	$\frac{1}{\sqrt{2}} \sum_{p\sigma} \sigma c_{-p\bar{\sigma}} c_{p\sigma}$	$4K_1$	$-(g_{3\perp} + g_{4\perp})$
$\pi$	$\frac{1}{\sqrt{2}} \sum_{p\sigma} w_p c_{-p+Q\bar{\sigma}} c_{p\sigma}$	$4K_2$	$g_{1\perp} - g_{2\perp}$
$\eta$	$\frac{1}{\sqrt{2}} \sum_{p\sigma} \sigma c_{-p+Q\bar{\sigma}} c_{p\sigma}$	$4K_2$	$-(g_{1\perp} + g_{2\perp})$
CDW	$\sum_{p\sigma} c_{p\sigma}^\dagger c_{p+Q\sigma}$	$-4P_2$	$-(g_{1\perp} + g_{3\perp}) - g$
SDW	$\sum_{p\sigma} \sigma c_{p\sigma}^\dagger c_{p+Q\sigma}$	$-4P_2$	$g_{1\perp} + g_{3\perp} - g$
OAF	$i \sum_{p\sigma} w_p c_{p\sigma}^\dagger c_{p+Q\sigma}$	$-4P_2$	$-(g_{1\perp} - g_{3\perp}) - g$
SN	$i \sum_{p\sigma} \sigma w_p c_{p\sigma}^\dagger c_{p+Q\sigma}$	$-4P_2$	$(g_{1\perp} - g_{3\perp}) - g$
FM	$\sum_{p\sigma} \sigma c_{p\sigma}^\dagger c_{p\sigma}$	$-4P_1$	$g_{2\perp} + g_{4\perp} + g$
PS	$\sum_{p\sigma} c_{p\sigma}^\dagger c_{p\sigma}$	$-4P_1$	$-(g_{2\perp} + g_{4\perp}) + g$

Fig. 16. Operator  $\hat{O}_\nu$ , bare response function  $R_\nu^0 (> 0)$  and coupling constant  $g_\nu$  for each correlation  $\nu$ . Each response function can be divergent (or there exists mean-field solution  $< \hat{O}_\nu > \neq 0$ ) for  $g_\nu > 0$ .  $g$  is defined as  $g \equiv g_{1\parallel} - g_{2\parallel}$ . In the RG method where only electrons near the saddle points are taken into account, the sum over  $p$  is restricted to  $p \sim (\pi, 0)$ ,  $(0, \pi)$  and the  $p$ -dependence of the  $d_{x^2-y^2}$ -wave factor  $w_p \propto \cos p_x - \cos p_y$  is ignored. In our calculation, we take  $w_p = \text{sgn}(\cos p_x - \cos p_y)$ .

can be rewritten as follows,

$$H_U = \frac{U}{2} \sum_i n_i n_i - \frac{U}{2} \sum_i n_i. \quad (4.15)$$

If we regard the second term in the r.h.s of eq. (4.15) as the chemical potential shift, we can take  $g_{i\perp}^0 = g_{i\parallel}^0 = U$  as the initial conditions and therefore use eq. (4.10) as the scaling equations of the coupling constants. For the perfect nesting case  $r \equiv |t'|/t = 0$ , Schulz<sup>28)</sup> and Dzyaloshinskii<sup>25)</sup> showed that SDW occurs, and pointed out that small deviations from half filling lead to dSC. Lederer *et al.*<sup>29)</sup> and Furukawa *et al.*<sup>33)</sup> solved the scaling equations for  $r \ll 1$  and the same results. Especially, Furukawa *et al.*<sup>33)</sup> indicated that the correlation of  $\pi$ -triplet pair is suppressed to zero. In these calculations, however,  $P_1$  and  $K_2$  are neglected in eq. (4.10) for the reason that they are less singular than  $P_2$ , i.e.,  $c, c'' \ll c'$  for  $r \ll 1$ , in eq. (4.5) and (4.6). On the other hand, Alvarez *et al.*<sup>31)</sup> solved the flow equations with the initial condition  $g_{i\perp}^0 = U$  and  $g_{i\parallel}^0 = 0$ , by neglecting the generation of  $g_{i\parallel}$  and omitting particle-particle diagram  $K_1$  and  $K_2$  in eq. (4.8), and showed that dSC, SDW and FM can be stabilized depending on  $U/t$  and  $r$ .

Now, we show the phase diagram in the plane of  $U > 0$  and  $V$  for  $t' = -1/5$  in Fig. 17, in which the ordered state with highest onset temperature is shown. First, we discuss the case that each ordered state is treated independently, because we cannot examine the coexistence of different orders in the RG method. The crucial difference from our mean field result is that superconductivity appears even for  $U > 0$  and  $V \geq 0$ , i.e., dSC for  $U > 4V$  and sSC for  $U < 4V$ . This result that dSC is possible for small  $V > 0$  as well as  $V = 0$  near half filling is consistent with a recent calculation based on the fluctuation-exchange (FLEX) approximation.<sup>36)</sup> Except for superconductivity for  $U > 0$  and  $V \geq 0$ , the RG phase diagram is qualitatively same as the mean field one when we do not take the coexistence of different orders into account, i.e., SDW and CDW appear for  $U > 4V$  and  $U < 4V$ , respectively, and attractive  $V < 0$  favors



dSC for small  $|V|$  and PS for large  $|V|$ , respectively. With regard to the correlation of  $\pi$ -triplet pair, our RG calculation has shown that it can be divergent for attractive  $V < 0$  and large  $|V|$  but is always subdominant. Similarly, FM cannot be the most dominant solely. These results are also consistent with our mean field ones.

Next, we discuss the possibility of the coexistence of different orders at low temperature, especially at  $T = 0$ . It is very important that our RG calculation shows the existence of a region where the onset temperature of SDW or CDW becomes highest, as shown in Fig. 17. Since our mean field calculation in §3.1 or §3.2 shows that the Fermi surface remains in the SDW and CDW states near half filling, we might expect to find a second phase transition at lower temperature in such SDW and CDW states. Therefore, at lower temperature in the SDW region in Fig. 17, (1) the coexistent state with dSC, SDW and  $\pi$ -triplet pair found for  $V < 0$  in the mean field approximation might be expected to survive for not only  $V < 0$  but also  $V \geq 0$ , and (2) the ferrimagnetic coexistent state with CDW, SDW and FM found for  $U > 4V > 0$  in the mean field approximation might be expected to survive. In fact, as we have pointed out in §3.1, VMC calculations for  $U > 0$  and  $V = 0$  show the coexistence of dSC and SDW at low temperature,<sup>13,15</sup> although  $\pi$ -triplet pair has been neglected. Similarly, at lower temperature in the CDW region in Fig. 17, (3) the ferrimagnetic coexistent state with CDW, SDW and FM found for  $4V > U > 0$  in the mean field approximation might be expected to survive. Especially,  $\pi$ -triplet pair (FM), which cannot be stabilized solely in the parameter region considered in the present mean field and RG approximation, might be expected to arise as a result of the coexistence of dSC and SDW (CDW and SDW). In order to assess the effect of  $\pi$ -triplet pair (FM) on the coexistence of dSC and SDW (CDW and SDW), we need another theoretical treatment.

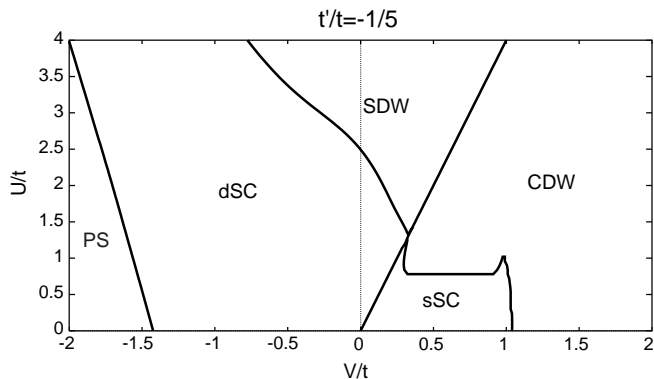


Fig. 17. The RG phase diagram for  $t'/t = -1/5$  and  $\mu = 4t'$ .

Here, we refer to the possibility of the coexistence of sSC and CDW. In the g-ology model in I, it can be easily shown that the coexistent state with sSC, CDW and  $\eta$ -singlet pair can be stabilized near half filling at low temperature for  $g_{3\perp} < 0$  and  $g_{1\perp} < 0$ .<sup>6</sup> As seen from eq. (2.2), this case corresponds to that of  $U < 0$  and  $V > 0$

in the present extended Hubbard model. Therefore, this coexistent state might be expected to be stabilized also in the extended Hubbard model for  $U < 0$  and  $V > 0$  in the mean field approximation. Moreover, based on the above discussion, it might be expected to survive in the presence of fluctuation for not only  $U < 0$  but also  $U \geq 0$ , at lower temperature in the CDW region in Fig. 17. This will be reported elsewhere.

Finally, we refer to the ambiguities of the above RG method. Since there exist not only log- but also  $\log^2$ -divergence in the particle-particle and particle-hole correlation functions, eq. (4.5), we cannot safely take the limit  $\omega \rightarrow 0$  in the scaling equations of coupling constants and response functions, eq. (4.8) and (4.13), i.e., it is not clear at all whether the above RG treatment is valid or not. In fact, the solution of eq. (4.8) and (4.13) depends on the initial value  $x_i$ . If we consider only the most singular  $\log^2$  term in  $K_1$  (and  $P_2$  for  $r = 0$ ) and take  $y \equiv x^2 = \log^2 \frac{E_c}{\omega}$  as a new scaling variable,<sup>28</sup> we can safely take  $\omega \rightarrow 0$  limit in the scaling equations of coupling constants. In this case, the above RG method might correspond to a parquet summation of leading  $\log^2$  divergences, rather than renormalization procedure.<sup>37</sup>

## §5. Conclusion and Discussion

We have studied in detail possible ordered states, especially possible coexistence of different orders, near half filling in the 2D extended Hubbard model with on-site repulsion  $U > 0$  and nearest-neighbor interaction  $V$ , with emphasis on electrons around the saddle points  $(\pi, 0)$  and  $(0, \pi)$ .

First, we have determined the phase diagram at  $T = 0$  in the mean field approximation. For  $V < 0$ , we have shown that the coexistent state with dSC, SDW and  $\pi$ -triplet pair can be stabilized near half filling. Here, we have indicated the following important fact which has often been neglected in previous studies: *when we discuss the coexistence of dSC and SDW, it is necessary to take  $\pi$ -triplet pair into account from the outset, because in general the coexistence of dSC and SDW results in  $\pi$ -triplet pair and is affected by  $\pi$ -triplet pair.*<sup>1</sup> Especially,  $\pi$ -triplet pair, which cannot condensate solely in the present model, can arise through the coexistence of dSC and SDW. Since the phase separation (PS) is generally expected to occur in the presence of finite-range attractive interaction such as  $V < 0$ , we have examined the effect of PS on the mean field ground state in the random phase approximation (RPA). The coexistent state with dSC, SDW and  $\pi$ -triplet pair is severely hampered by PS but survives, and that the long-range Coulomb repulsion such as next-nearest-neighbor density-density repulsion leads to the suppression of PS. On the other hand, for  $V > 0$ , we showed that a *ferrimagnetic* coexistent state with commensurate charge-density-wave (CDW), SDW and ferromagnetism (FM) can be stabilized near half filling. Here, we have indicated the following important fact: *when we discuss the coexistence of CDW and SDW, it is necessary to take FM into account from the outset, because in general the coexistence of CDW and SDW results in FM and is affected by FM.* Especially, FM, which cannot be stabilized solely with

the present choice of parameters, can arise through the coexistence of CDW and SDW. It is to be noted that the above mean field coexistent states near half filling can be stabilized at low temperature, especially at  $T = 0$ , when CDW or SDW, in which the Fermi surface remains near half filling, arises first at high temperature.

In order to examine the effects of fluctuation on the mean field ordered states, we have adopted the RG method for the *special* case that the Fermi level lies just on the saddle points. We have shown that the crucial difference from our mean field result is that superconductivity can arise even for  $U > 0$  and  $V \geq 0$ ; dSC and sSC for  $U > 4V$  and  $U < 4V$ , respectively. Except for this difference, the RG phase diagram is qualitatively same as the mean field one when we do not take the coexistence of different orders into account, *e.g.*, SDW and CDW can arise for  $U > 4V$  and  $U < 4V$ , respectively. Especially, the correlation of  $\pi$ -triplet pair or FM cannot be the most dominant solely. Here, it is very important that a region where the onset temperature of SDW or CDW becomes highest is found in the RG phase diagram. Since the Fermi surface remains near half filling in these SDW and CDW states, we might expect to find a second phase transition at lower temperature. In the RG method, however, we cannot assess such possibilities. On the other hand, the mean field approximation, which is often questionable for the 2D case, is of great advantage in that we can study the stability of coexistent states with different order parameters quantitatively. Therefore, we can conclude that our mean field calculations indicate the possibilities that (1) SDW, which has been shown in our RG calculation to arise first at high temperature for  $U > 4V$ , coexists with dSC *and*  $\pi$ -triplet pair, or with CDW *and* FM, at lower temperature, and that (2) CDW, which has been shown in our RG calculation to arise first at high temperature for  $U < 4V$ , coexists with SDW *and* FM, at lower temperature.

Throughout this letter, we have assumed YBCO-type Fermi surface by introducing  $t'$  and consider only *commensurate* (C) SDW or CDW. Near half filling, however, *incommensurate* (IC) ordering or stripe formation can be expected, especially for  $t' = 0$  in the repulsive Hubbard model.<sup>38,39,40</sup> Recently, the effect of  $V$  on such stripe states has been examined.<sup>41</sup> The effect of IC ordering on the stability of the coexistent states (with dSC, C-SDW and  $\pi$ -triplet pair, and with C-CDW, C-SDW and FM) is beyond the scope of the present study. In the repulsive Hubbard model with  $t' = 0$ , Giamarchi *et al.*<sup>42</sup> have shown that the coexistent state with dSC and C-SDW state have higher energy than that with dSC and IC-SDW.

With regard to dSC, we have assumed that the superconducting gap symmetry is purely of  $d_{x^2-y^2}$ -wave. However, there are a few indications that dSC mixed with components of other symmetry can be stabilized,<sup>5,43,44,45</sup> dependent on interaction, electron density, etc. Such mixed pairing states leave much room for future studies.

The author thanks to H. Fukuyama, H. Kohno and M. Ogata for valuable discussions.

## Appendix A: Symmetry among Various Order Parameters

We examine the relationship among the order parameters as shown in Fig. 16. First, the operators of dSC, SDW and  $\pi$ -triplet pair are equivalent in that they are 'rotated' into each other,

$$[\hat{O}_{SDW}, \hat{O}_{dSC}] = 2\hat{O}_\pi, \quad [\hat{O}_\pi^\dagger, \hat{O}_{SDW}] = 2\hat{O}_{dSC}^\dagger, \quad (\text{A}\cdot 1\text{a})$$

$$[\hat{O}_{dSC}, \hat{O}_\pi^\dagger] = 2\hat{O}_{SDW}. \quad (\text{A}\cdot 1\text{b})$$

This relationship underlies the  $SO(5)$  theory, in which dSC and SDW are unified into a *five*-dimensional vector *superspin* and  $\hat{O}_\pi$  describes excitation towards the SDW (dSC) direction in the dSC (SDW) ground state.<sup>8</sup> We note that eq. (A.1b) holds due to  $w_p^2 = 1$ , *i.e.*,  $w_p \equiv \text{sgn}(\cos p_x - \cos p_y)$ . If  $w_p \propto \cos p_x - \cos p_y$ , it is satisfied only in the long wavelength limit where only electrons near the saddle points are important. It is very important to note that if two of the above three order parameters coexist, another one also results generally. As we have already shown in the mean field approximation, the coexistent state with dSC, SDW *and*  $\pi$ -triplet pair can be stabilized near half filling in the 2D extended Hubbard model for  $U > 0$  and  $V < 0$ .

Next, the operators of sSC, CDW and  $\eta$ -singlet pair are equivalent in that they are 'rotated' into each other,

$$[\hat{O}_{CDW}, \hat{O}_{sSC}^\dagger] = 2\hat{O}_\eta^\dagger, \quad [\hat{O}_\eta, \hat{O}_{CDW}] = 2\hat{O}_{sSC}, \quad (\text{A}\cdot 2\text{a})$$

$$[\hat{O}_{sSC}^\dagger, \hat{O}_\eta] = 2\hat{O}_{CDW}, \quad (\text{A}\cdot 2\text{b})$$

This relationship underlies the  $SO(3)$  theory, in which sSC and CDW are unified into a *three*-dimensional vector *pseudospin* and  $\hat{O}_\eta$  describes excitation towards the CDW (sSC) direction in the sSC (CDW) ground state.<sup>34,35</sup> In fact, such properties are useful in the *attractive* Hubbard model. It is very important to note that if two of the above three order parameters coexist, another one also results generally. It can be easily shown in the mean field approximation that a state where sSC, CDW *and*  $\eta$ -singlet pair coexist can be stabilized near half filling in the  $g$ -ology model used in I for  $g_{3\perp} < 0$  and  $g_{1\perp} < 0$ .<sup>6</sup>

We note that similar relationships hold among dSC, OAF and  $\eta$ -singlet pair,

$$[\hat{O}_\eta^\dagger, \hat{O}_{dSC}] = 2i\hat{O}_{OAF}, \quad [\hat{O}_{OAF}, \hat{O}_\eta] = 2i\hat{O}_{dSC}, \quad (\text{A}\cdot 3\text{a})$$

$$[\hat{O}_{dSC}^\dagger, \hat{O}_{OAF}] = 2i\hat{O}_\eta^\dagger, \quad (\text{A}\cdot 3\text{b})$$

and among sSC, SN and  $\pi$ -triplet pair,

$$[\hat{O}_{sSC}^\dagger, \hat{O}_\pi] = 2i\hat{O}_{SN}, \quad [\hat{O}_{SN}, \hat{O}_{sSC}] = 2i\hat{O}_\pi, \quad (\text{A}\cdot 4\text{a})$$

$$[\hat{O}_\pi^\dagger, \hat{O}_{SN}] = 2i\hat{O}_{sSC}^\dagger. \quad (\text{A}\cdot 4\text{b})$$

If  $w_p \propto \cos p_x - \cos p_y$ , eq. (A.3b) and (A.4b) hold only approximately. In each case, if two of the above three order parameters coexist, another one also results generally. It can be easily shown in the mean field ap-

proximation that a state where dSC, OAF and  $\eta$ -singlet pair (sSC, SN and  $\pi$ -triplet pair) coexist can be stabilized in the g-ology model used in I for  $g_{3\perp} > 0$  and  $g_{1\perp} < 0$  ( $g_{3\perp} < 0$  and  $g_{1\perp} > 0$ ).<sup>6</sup>

Moreover, eq. (A.1)-(A.4) imply close relationships (1) between sSC and dSC, (2) between  $\eta$ -singlet pair and  $\pi$ -triplet pair, and (3) between density-wave (CDW, SDW) and local-current (OAF, SN). In fact, the *hermite* operators of uniform bond-charge and bond-spin (BC and BS) density with  $d_{x^2-y^2}$ -symmetry defined as

$$\hat{O}_{BC} = \sum_{p\sigma} w_p c_{p\sigma}^\dagger c_{p\sigma}, \quad \hat{O}_{BS} = \sum_{p\sigma} \sigma w_p c_{p\sigma}^\dagger c_{p\sigma}, \quad (\text{A.5})$$

satisfy similar commutation relations,

$$[\hat{O}_\alpha^\dagger, \hat{O}_\beta] = 2\hat{O}_\gamma, \quad [\hat{O}_\gamma, \hat{O}_\alpha^\dagger] = 2\hat{O}_\beta^\dagger, \quad (\text{A.6a})$$

$$[\hat{O}_\beta, \hat{O}_\gamma] = 2\hat{O}_\alpha, \quad (\text{A.6b})$$

for  $(\alpha, \beta, \gamma) = (\text{sSC}, \text{dSC}, \text{BC})$  and  $(\eta, \pi, \text{BS})$ , and

$$[\hat{O}_\alpha, \hat{O}_\beta] = 2i\hat{O}_\gamma, \quad [\hat{O}_\gamma, \hat{O}_\alpha] = 2i\hat{O}_\beta, \quad (\text{A.7a})$$

$$[\hat{O}_\beta, \hat{O}_\gamma] = 2i\hat{O}_\alpha, \quad (\text{A.7b})$$

for  $(\alpha, \beta, \gamma) = (\text{SDW}, \text{BC}, \text{SN}), (\text{CDW}, \text{BC}, \text{OAF}), (\text{SDW}, \text{BS}, \text{OAF})$  and  $(\text{CDW}, \text{BS}, \text{SN})$ . If  $w_p \propto \cos p_x - \cos p_y$ , eq. (A.6b) and (A.7b) hold only approximately in each case.

The relationship among order parameters which are rotated into each other by  $\hat{O}_\eta, \hat{O}_\pi, \hat{O}_{BC}$  and  $\hat{O}_{BS}$  is summarized as shown in Fig. 18, where the connection with  $\hat{O}_{dSC}$  and  $\hat{O}_{sSC}$  by  $\hat{O}_{BC}$  is not explicitly shown.

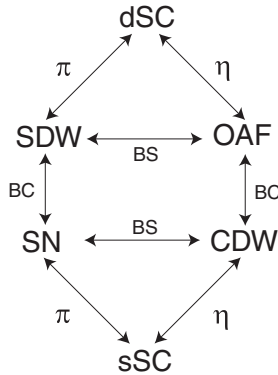


Fig. 18. The relationship among various order parameters.

## Appendix B: Charge Susceptibility in the Random Phase Approximation

The charge compressibility  $\kappa$  is equal to static and uniform charge susceptibility  $\chi$ ,

$$\kappa = \lim_{q \rightarrow 0} \chi^R(q, q, \omega = 0), \quad (\text{B.1})$$

where  $\chi^R(q, q', \omega)$  is the retarded density-density correlation function, which is obtained from the analytic con-

tinuation of  $\chi(q, q', i\omega_l)$  through  $i\omega_l \rightarrow \omega + i\delta$ ,

$$\chi(q, q', i\omega_l) = \int_0^\beta d\tau e^{i\omega_l \tau} \chi(q, q', \tau). \quad (\text{B.2a})$$

$\chi(q, q', \tau)$  is the two-particle thermal Green function in imaginary time given by

$$\chi(q, q', \tau) = \sum_{\sigma\sigma'} N_{\sigma\sigma'}(q, q', \tau), \quad (\text{B.3a})$$

$$N_{\sigma\sigma'}(q, q', \tau) = \frac{1}{N} \langle T_\tau n_{q\sigma}(\tau) n_{-q'\sigma'} \rangle, \quad (\text{B.3b})$$

where  $n_{q\sigma} = \sum_k c_{k\sigma}^\dagger c_{k+q\sigma}$ ,  $n_{-q\sigma} = (n_{q\sigma})^\dagger$ . We write  $N_{\sigma\sigma'}$  in the matrix form as follows,

$$\hat{N} = \begin{pmatrix} N_{\uparrow\uparrow} & N_{\uparrow\downarrow} \\ N_{\downarrow\uparrow} & N_{\downarrow\downarrow} \end{pmatrix}. \quad (\text{B.4})$$

For the mean field Hamiltonian with  $\Delta_{dSC}, \Delta_{SDW}$  and  $\Delta_\pi$ , the one-particle thermal Green functions, defined by

$$G_{\sigma\sigma'}(p, p', \tau) \equiv - \langle T_\tau c_{p\sigma}(\tau) c_{p'\sigma'}^\dagger \rangle, \quad (\text{B.5a})$$

$$F_{\sigma\sigma'}^\dagger(p, p', \tau) \equiv - \langle T_\tau c_{p\sigma}^\dagger(\tau) c_{p'\sigma'} \rangle, \quad (\text{B.5b})$$

$$F_{\sigma\sigma'}(p, p', \tau) \equiv - \langle T_\tau c_{p\sigma}(\tau) c_{p'\sigma'} \rangle, \quad (\text{B.5c})$$

have the following form,

$$G_{\sigma\sigma}(p, p', \tau) \equiv \delta_{p',p} G_{\sigma\sigma 1}(p, \tau) + \delta_{p',p+Q} G_{\sigma\sigma 2}(p, \tau), \quad (\text{B.6a})$$

$$F_{\sigma\bar{\sigma}}^{(\dagger)}(p, p', \tau) \equiv \delta_{p',-p} F_{\sigma\bar{\sigma} 1}^{(\dagger)}(p, \tau) + \delta_{p',-p+Q} F_{\sigma\bar{\sigma} 2}^{(\dagger)}(p, \tau). \quad (\text{B.6b})$$

Therefore, it is seen that  $\hat{\chi}$  has the following form,

$$\hat{N}(q, q', \tau) = \delta_{q',q} \hat{N}_1(q, \tau) + \delta_{q',q+Q} \hat{N}_2(q, \tau), \quad (\text{B.7a})$$

$$\hat{N}_1 = \begin{pmatrix} N_{1\parallel} & N_{1\perp} \\ N_{1\perp} & N_{1\parallel} \end{pmatrix}, \quad (\text{B.7b})$$

$$\hat{N}_2 = \begin{pmatrix} N_{2\parallel} & N_{2\perp} \\ -N_{2\perp} & -N_{2\parallel} \end{pmatrix}, \quad (\text{B.7c})$$

The subscript 1 and 2 represent normal and Umklapp part, respectively. It is to be noted that there exists Umklapp part  $\hat{N}_2$  for  $\Delta_{SDW} \neq 0$  or  $\Delta_\pi \neq 0$ . With regard to  $\chi(q, q', \tau)$ , it has only normal part,

$$\chi(q, q', \tau) = \delta_{q',q} \chi_0(q, \tau), \quad (\text{B.8a})$$

$$\chi_0(q, \tau) \equiv 2 \{ N_{1\parallel}(q, \tau) + N_{1\perp}(q, \tau) \}. \quad (\text{B.8b})$$

Next, we treat the effect of interaction in the random phase approximation (RPA). The RPA equation is diagrammatically shown in Fig. 19. Here, we consider only (a) for interaction vertex in Fig. 19, which leads to the diagram shown in Fig. 3. In the frequency space, the RPA equation is written as follows ( $z \equiv i\omega_l$ ),

$$\hat{N}_{RPA}(q, q', z) = \hat{N}(q, q', z) + \sum_{q_1} \hat{N}(q, q_1, z) \hat{g}(q_1) \hat{N}_{RPA}(q_1, q', z), \quad (\text{B.9a})$$

where

$$\hat{g} \equiv \begin{pmatrix} g_{\parallel} & g_{\perp} \\ g_{\perp} & g_{\parallel} \end{pmatrix}, \quad (\text{B.9b})$$

$$g_{\parallel}(q) \equiv -2V_q, \quad g_{\perp}(q) \equiv -(U + 2V_q), \quad (\text{B}\cdot\text{9c})$$

and  $V_q = V(\cos q_x + \cos q_y)$ . Since it can be seen that  $\tilde{N}_{RPA}$  has the same form as eq. (B-7),  $\chi_{RPA}$  is obtained as follows,

$$\chi_{RPA}(q, q) = 2 \frac{n_q^+ X_{q+Q}^- + Y_q}{X_q^+ X_{q+Q}^- - g_q^+ Y_q}, \quad (\text{B}\cdot\text{10a})$$

$$\chi_{RPA}(q, q+Q) \equiv 0, \quad (\text{B}\cdot\text{10b})$$

where

$$n_q^{\pm} \equiv N_{1\parallel}(q) \pm N_{1\perp}(q), \quad u_q^{\pm} \equiv N_{2\parallel}(q) \pm N_{2\perp}(q), \quad (\text{B}\cdot\text{10c})$$

$$g_q^{\pm} \equiv g_{\parallel}(q) \pm g_{\perp}(q), \quad (\text{B}\cdot\text{10d})$$

$$X_q^{\pm} = 1 - g_q^{\pm} n_q^{\pm}, \quad Y_q = g_{q+Q}^- u_q^- u_{q+Q}^+, \quad (\text{B}\cdot\text{10e})$$

and the variable  $z$  is not explicitly written. Therefore, we can obtain the charge compressibility  $\kappa$  in the RPA, from eq. (B-1) and (B-10a). In the normal or dSC state,  $\chi_{RPA}$  has a familiar form due to  $u_q^{\pm} \equiv 0$ ,

$$\chi_{RPA}(q, q) = \frac{2n_q^+}{X_q^+} = \frac{\chi_0(q)}{1 + \frac{1}{2}(U + 4V_q)\chi_0(q)}, \quad (\text{B}\cdot\text{11})$$

where  $\chi_0$  is given by eq. (B-8b). However, since  $u_q^{\pm} \neq 0$  in the SDW or  $\pi$ -triplet pairing state, especially in the coexistent state with dSC, SDW and  $\pi$ -triplet pair,  $\chi_{RPA}$  has a nontrivial form.

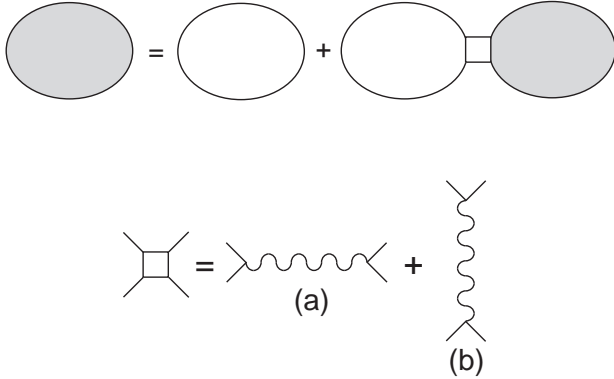


Fig. 19. The RPA equation for charge susceptibility. The square stands for interaction vertex. In our calculation, the diagram of (b) for interaction vertex is neglected.

[1] M. Murakami and H. Fukuyama: J. Phys. Soc. Jpn. **67** (1998) 41; 2784.  
 [2] R. Micnas, J. Ranninger, S. Robaszkiewicz and S. Tabor: Phys. Rev. B **37** (1988) 9410; R. Micnas, J. Ranninger and S. Robaszkiewicz: Phys. Rev. B **39** (1989) 11653; R. Micnas, J. Ranninger and S. Robaszkiewicz: Rev. Mod. Phys. **62** (1990) 114.  
 [3] E. Dagotto, J. Riera, Y. C. Chen, A. Moreo, A. Nazarenko, F. Alcaraz and F. Ortolani: Phys. Rev. B **49** (1994) 3548; A. Nazarenko, A. Moreo, E. Dagotto and J. Riera: Phys. Rev. B **54** (1996) R768.  
 [4] J. Ferrer, M. A. González-Alvarez and J. Sánchez-Cañizares: Phys. Rev. B **57** (1998) 7470.  
 [5] J. F. Annett and J. P. Wallington: condmat/9807220.

[6] M. Murakami: Ph.D. thesis (1998).  
 [7] E. Demler and S. C. Zhang: Phys. Rev. Lett. **75** (1995) 4126.  
 [8] S. C. Zhang: Science **275** (1997) 1089.  
 [9] L. Arrachea and A. A. Aligia: Physica C **303** (1998) 141.  
 [10] G. C. Psaltakis and E. W. Fenton: J. Phys. C **16** (1983) 3913.  
 [11] M. Inaba, H. Matsukawa, M. Saitoh and H. Fukuyama: Physica C **257** (1996) 299.  
 [12] G. J. Chen, R. Joynt, F. C. Zhang and C. Gros: Phys. Rev. B **42** (1990) 2662.  
 [13] T. Giamarchi and C. Lhuillier: Phys. Rev. B **43** (1991) 12943.  
 [14] A. Himeda and M. Ogata: Phys. Rev. B **60** (1999) R9935.  
 [15] K. Yamaji, T. Yanagisawa, T. Nakanishi and S. Koike: Physica C **304** (1998) 225.  
 [16] S. Kivelson, W. -P. Su, J. R. Schrieffer and A. J. Heeger: Phys. Rev. Lett. **58** (1987) 1899.  
 [17] J. E. Hirsch: Physica C **158** (1989) 326.  
 [18] D. K. Campbell, J. Tinka Gammel and E. Y. Loh, Jr.: Phys. Rev. B **42** (1990) 475.  
 [19] F. Marsiglio and J. E. Hirsch: Phys. Rev. B **49** (1994) 1366.  
 [20] I. Affleck and J. B. Marston: Phys. Rev. B **37** (1988) 3774.  
 [21] H. J. Schulz: Phys. Rev. B **39** (1988) 2940.  
 [22] A. A. Nersesyan and G. E. Vachnadze: J. Low Temp. Phys. **77** (1989) 293.  
 [23] A. A. Nersesyan, G. I. Japaridze and I. G. Kimeridze: J. Phys. Condens. Matter **3** (1991) 3353.  
 [24] B. Chattopadhyay and D. M. Gaitonde: Phys. Rev. B **55** (1997) 15364.  
 [25] I. E. Dzyaloshinskii: Zh. Eksp. Teor. Fiz. **93** (1987) 1487 [Sov. Phys. JETP **66** (1987) 848].  
 [26] N. Kobayashi, M. Ogata and K. Yonemitsu: J. Phys. Soc. Jpn. **67** (1998) 1098.  
 [27] D. R. Penn: Phys. Rev. **142** (1966) 350.  
 [28] H. J. Schulz: Europhys. Lett. **4** (1987) 609.  
 [29] P. Lederer, G. Montambaux and D. Poilblanc: J. Physique **48** (1987) 1613.  
 [30] J. González, F. Guinea and M. A. H. Vozmediano: Europhys. Lett. **34** (1996) 711; Nucl. Phys. B **485** (1997) 694.  
 [31] J. V. Alvarez, J. González, F. Guinea and M. A. H. Vozmediano: J. Phys. Soc. Jpn. **67** (1998) 1868; condmat/9804153.  
 [32] J. V. Alvarez and J. González: condmat/9803131.  
 [33] N. Furukawa, T. M. Rice and M. Salmhofer: Phys. Rev. Lett. **81** (1998) 3195.  
 [34] C. N. Yang: Phys. Rev. Lett. **63** (1989) 2144.  
 [35] S. C. Zhang: Phys. Rev. Lett. **65** (1990) 120; Int. J. Mod. Phys. B **5** (1991) 153.  
 [36] G. Esirgen, H. -B. Schüttler and N. E. Bickers: Phys. Rev. Lett. **82** (1999) 1217.  
 [37] J. González, F. Guinea and M. A. H. Vozmediano: condmat/9905166.  
 [38] H. J. Schulz: Phys. Rev. Lett. **64** (1990) 1445.  
 [39] D. Poilblanc and T. M. Rice: Phys. Rev. B **39** (1989) 9749.  
 [40] M. Kato, K. Machida, H. Nakanishi and M. Fujita: J. Phys. Soc. Jpn. **59** (1990) 1047.  
 [41] G. Seibold, C. Castellani, C. Di. Castro and M. Grilli: Phys. Rev. B **58** (1998) 13506.  
 [42] T. Giamarchi and C. Lhuillier: Phys. Rev. B **42** (1990) 10641.  
 [43] R. B. Laughlin: Phys. Rev. Lett. **80** (1998) 5188.  
 [44] M. Ogata: J. Phys. Soc. Jpn. **66** (1997) 3375.  
 [45] K. Kuroki and H. Aoki: J. Phys. Soc. Jpn. **67** (1998) 1533.